Force of Adhesion Upon Loss of Contact Angle Hysteresis: When a Liquid Behaves Like a Solid

Juan V. Escobar* and Rolando Castillo

Instituto de Física, Universidad Nacional Autónoma de México, P. O. Box 20-364, Mexico City 04510, Mexico

(Received 19 August 2013; published 27 November 2013)

The theoretically predicted vanishment of the macroscopic contact angle hysteresis is found experimentally along with a small but finite force of adhesion ($F_{\mathrm{Ad}} \approx -0.5\ \mu$N) that, unexpectedly, is independent of the history of the preload. Our results agree with the prediction of a model in which the surface tension of the liquid provides the counterpart of the restoring force of an elastic solid, evidencing that the dewetting of a liquid in the absence of strong pinning points is equivalent to the detachment of an elastic solid.

DOI: 10.1103/PhysRevLett.111.226102 PACS numbers: 68.08.Bc, 46.55.+d, 81.05.ug

When an elastic solid sphere of radius R is pressed against a surface and subsequently detached from it, a counterintuitive result is found: the force of adhesion or "pull-off force" ($F_{\mathrm{Ad}}^{\mathrm{Solid}}$) is not only independent of the Young's moduli of the bodies, but also of the history of the compression. In other words, the compression or decompression process is completely reversible, and yet, a small but finite constant $F_{\mathrm{Ad}}^{\mathrm{Solid}}$ is measured [1–5] that is proportional to the work of adhesion, w_a:

$$F_{\mathrm{Ad}}^{\mathrm{Solid}} \propto -\pi R w_a. \tag{1}$$

This reversibility contrasts sharply with what is usually found in the interaction between liquids and surfaces [6]. There, either surface roughness or patches with chemical inhomogeneities of higher local wettability result in contact angle hysteresis [7] (CAH). The force arising from the elastic deformation of the pinned contact line at these points opposes the detachment of the liquid from the surface. Thus, it is normally expected that wetting be a hysteretic process. Although vanishment of the force hysteresis has been recently measured on individual pinning points [8], as we show in the present work the contact with of a collection of such points in a macroscopic experiment does not yield a total zero adhesion. Our system of study is comprised of a submillimeter semidrop of mercury (Hg) in contact with a boron doped diamond surface treated to be super-mercury-phobic. The effective surface energy of this liquid-solid system is so low ($\approx 2\ \mathrm{mJ/m^2}$) that there is no pinning of the contact line. As a consequence, the CAH vanishes and yet, a finite force of adhesion independent of the history of the compression is measured [Fig. 1(l)], just as in the case of the contact between elastic solids. We use a similar energy balance as the one put forward by Johnson-Kendall-Roberts (JKR) [3] of the deformation of soft elastic solids, leading to a parameter-free prediction of a constant force of adhesion between Hg and a super-mercury-phobic surface. Our results imply that the dewetting process of Hg from this surface is equivalent to the detachment of an elastic solid, thus bringing further together two once perceived separate areas of study: Surface physics and mechanics [4].

The top row in Fig. 1 shows Hg drops resting on three surfaces of increasing roughness. The high surface tension of mercury ($\gamma_{lv} = 486.5\ \mathrm{mJ/m^2}$) yields a very steep equilibrium contact angle with the flat surface [$\theta_E = 155°$, Fig. 1(a)], an ideal starting point for achieving a roughness-induced state of supersolvophobicity [6,9]. Indeed, a rough microcrystalline boron doped diamond film with apparent contact angle $\theta^* = 162°$ [Fig. 1(b)] is rendered super-mercury-phobic [$\theta^* > 175°$, Fig. 1(c)] after a thermal oxidation process transforms the 10 $\mu\mathrm{m}^2$ crystals into pyramids with nanometer-scale tops [10]. Adhesion with mercury is so low, that Hg drops in free-fall form jets upon colliding with this surface [11]. In static contact, a Teflon ring is needed to prevent the mercury drop from spontaneously sliding out of the surface at an apparent zero-tilt angle, a predicted consequence of the vanishment of the CAH for rough surfaces [9]. As shown by Johnson and Dettre [12], increased roughness can reduce the CAH since the liquid becomes progressively more in contact with air than with the substrate itself (for $\theta_E > 90°$). Later, de Gennes and Joanny [7] pioneered the theoretical study of the conditions necessary to suppress CAH, and referred to the areas of higher local wettability as "pinning points" of the three phase contact line. In the exclusive presence of "weak" pinning points the CAH is expected to vanish, so that the compression or detachment process of a liquid drop should be completely reversible. The second row of Fig. 1 shows drops of Hg during their detachment from these surfaces. Note how, while the drop deforms considerably on both the polished and microcrystalline samples, on the oxidized one the drop's profile transitions smoothly from contact to noncontact in a seemingly perfectly reversible way. We thus expect no CAH on this surface (Fig. 3) and a much smaller force of adhesion that should not depend on the history of the contact.

Our force of adhesion experimental setup is depicted in Fig. 2 and consists of a custom-made force microscope [11,13] modified to be able to hold a macroscopic Hg

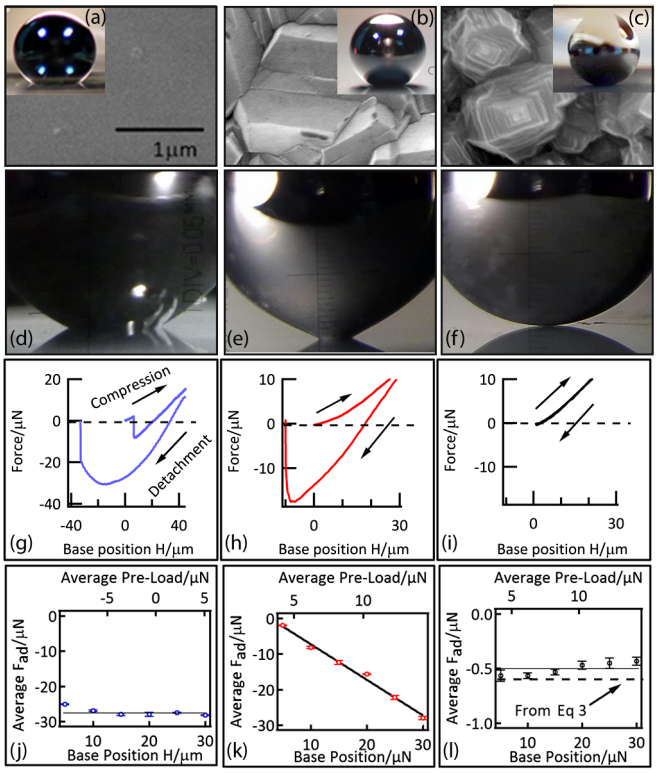

FIG. 1 (color online). Topography, contact angle, and force of adhesion results. (First row) Left-middle-right columns display SEM topography images of the polished-microcrystalline- nano-contact boron doped diamond surfaces. (Insets) 1mm drops of Hg resting on each surface. (Second row) Hg drops being detached from the corresponding surfaces. (Third row) Typical force data during compression or detachment cycles. (Fourth row) Corresponding average F_{Ad}. Standard deviations are 1%, 3%, and 7% for Figs. (j),(k), and (l), respectively. The line in Fig. 1(l) displays the prediction from a model of the interaction with a perfectly super-mercury-phobic surface [Eq. (3)] for an elastic solid of the same radius and effective w_a. Solid lines in Figs. (j),(l), and (k) depict the average and linear fit of the respective data.

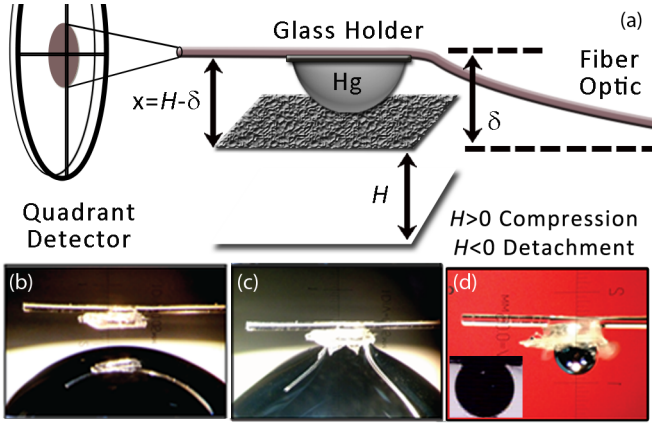

FIG. 2 (color online). Experimental setup: (b) A small, thin piece of glass covered with a sticky polymer is glued about 1 mm away from the end of a 7.5 mm-long fiber optic connected to an 830 nm diode laser (Thorlabs, USA) and pointing to a quadrant detector. The holder is brought in contact with a pool of mercury (c) then retracted, leaving a semidrop on its surface (d). (a) As the base holding the surfaces moves a distance H, the semidrop is compressed and the fiber is deflected a distance δ, yielding a force ($k\delta$), where k is the spring constant of the fiber (5.4 + / − 0.4 N/m). The magnitude of the compression is $x \equiv (H - \delta)$. The contact angle between the semidrop and the polymer (θ_p) remains fixed at about 120° after hundreds of compression or detachments tests [inset of Fig. 2(d)].

semidrop. To do so, we take advantage of the notoriously high adhesion that exists between sticky polymers and mercury [14] to stick an Hg semidrop of radius $R = 350\ \mu$m to a 1×1 mm^2 polymer-covered piece of glass, making a 120° contact angle (θ_p). The piece of glass is glued at the end of a fiber optic used as a force gauge.

An example of the experimental data is shown on the third row of Fig. 1. Note that there exists a large force hysteresis on the first two surfaces that is almost absent on the super-mercury-phobic one. The measured force of adhesion as a function of the displacement H of the base (or equivalently of the corresponding average preload) is presented for each surface at the bottom row of Fig. 1. It is striking that just as in the case of the contact between elastic solids, the force of adhesion on the super-mercury-phobic surface is constant. Consistent with this result, Fig. 3(b) shows that the CAH indeed vanishes, in contrast with the result on the microcrystalline film that is markedly hysteretic. This suggests that the interaction energy (E_s) between the semidrop and the oxidized surface is extremely low. To incorporate this surface term into a physical model, we follow Griffith [4,15] who recognized that surface interactions can couple with elasticity and influence contact dynamics. If we consider only short range interactions—such as the van der Waals (vdW) forces—the interaction energy is proportional to the energetic cost (w_a) of bringing apart a unit area of contacting surfaces [1,3]. Taking the value of γ_{lv} for mercury, and its contact angle with the flat diamond [$\theta_E = 155°$, Fig. 1(a)], the Dupré equation [6] yields $w_a = \gamma_{\mathrm{lv}}(1 + \cos\theta_E) = 45.55$ mJ/m^2, which falls within the expected values for the vdW interactions [16].

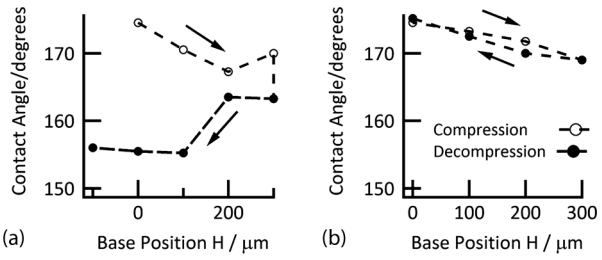

FIG. 3. CAH results: (a) Pronounced CAH on the microcrystalline sample and (b) vanishment of the CAH on the super-mercury-phobic one. A 2 mm Hg drop was used for these tests. See Supplemental Material [11] for details.

However, the actual interaction energy with the rough surface is much smaller than that with the polished one. Here we make the assumption that w_a diminishes in proportion to the so-called fractional surface area, ϕ_s, defined as the fraction of the surface in actual contact with the liquid [6] (the nanotops of the pyramids). This approximation is valid as long as the profile of the drop remains flat against the surface [17]. A wetting state in which the liquid is held only by a few points on the surface ("Fakir effect") was studied by Cassie and Baxter [18] and relates θ^* to ϕ_s and θ_E through the relation: $\cos\theta^* = -1 + \phi_s(1 + \cos\theta_E)$. The value of ϕ_s that accounts for the contact angle θ^* with the oxidized surface is 40×10^{-3}. Therefore, the effective surface energy is brought down to the very low value $w_a^e \equiv w_a\phi_s = 1.82$ mJ/m^2. In the theory of contact mechanics, the contribution from similar interactions limited to the area of contact were originally studied by Derjaguin [1] who assumed that the deformation of the surface remains Hertzian [19], and by the JKR model that incorporates the fact that adhesive forces may decrease the contact angle for soft materials. In our system, the equivalent to Derjaguin's model is the deformation of a semidrop against a perfectly mercury-phobic wall ($\theta^* = 180°$), and constitutes the zeroth order approximation to the real contact with the low energy surface. An evident difference between the deformation of liquid drops and solid spheres is that the former have no internal stresses, so that there is no classical elastic energy involved. However, a deformed drop will exhibit an equivalent restoring force supplied by the surface tension that tends to minimize the surface area of the liquid [Eq. (2)], giving rise to a spheroid [Fig. 4(a)]. The pseudo-elastic energy (E_E) associated with this deformation is given by the increase in surface area of the drop multiplied by $\gamma_{\rm lv}$. Both E_E and the contact energy ($E_s = w_a^e \pi a_0^2$; $a_0 \equiv$ radius of contact) can be calculated from the profile of the drop that minimizes ~~the surface area given by~~ the functional

$$\text{~~Area~~} = 2\pi \int_x^R \left(y[z]\sqrt{1 + (\partial_z y[z])^2} \right) dz - \lambda\pi \int_x^R y[z]^2 dz, \tag{2}$$

where $y[z]$ is the profile of the drop as a function of the coordinate z and λ is Lagrange's multiplier that ensures that the volume of the semidrop is conserved [6,11]. An assumption, verified experimentally, made to solve Eq. (2) is that the contact line is pinned while the contact angle varies during compression. The three different boundary conditions that arise are discussed in the Supplemental Material [11]. An example of the profile that satisfies Eq. (3) is shown in Fig. 4(a). The calculated E_E and E_s are very well fit to a power law $[2\pi R^2 S\gamma_{\rm lv}(x/R)^\beta$, with $\beta = 2.3$, Fig. 4(b)] and to a polynomial $[\pi R^2 w_a^e\{A(x/R)^2 + B(x/R)\}$, Fig. 4(c)] respectively, where S, A, and B are constants of order 1 that depend on the value of θ_p. The final term needed in the energy balance is the mechanical energy

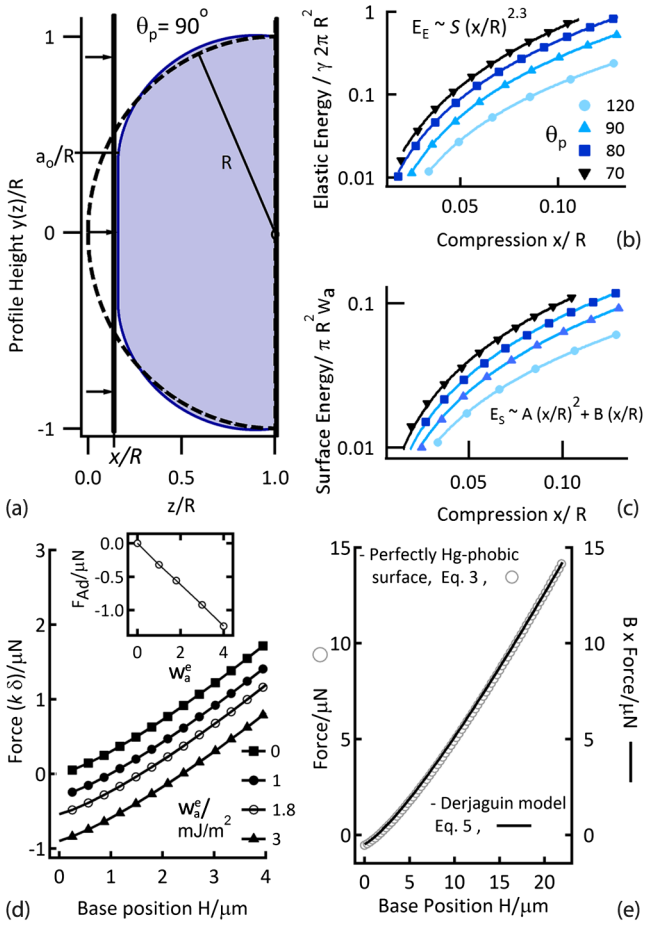

FIG. 4 (color online). (a) Theoretical profile of the deformed drop. (b,c) E_s and E_E vs (x/R) for different θ_p (if $\theta_p = 120°$, $A = 1.46$, $B = 0.28$ and $S = 0.26$). (d) Theoretical $F^{\rm Hg}(H)$ (Eq. (3) and $(dE_{Hg}/d\delta)_H = 0$) for different w_a^e and $\theta_p = 120°$. (inset) Corresponding $F_{\rm Ad}^{\rm Hg}$. (e) Reaction forces setting $w_a^e = 1.8$ mJ/m^2: Derjaguin model with $K = 65$ KPa (line) and perfectly Hg-phobic system (circles).

of the fiber, $E_m = (1/2)k\delta^2$. Using $x \equiv H - \delta$ (see Fig. 2), the total energy as a function of the deflection δ is then

$$E_{\rm Hg} \equiv E_E + E_m - E_s = \frac{k\delta^2}{2} + 2\pi R^2 S\gamma_{\rm lv}\left(\frac{H-\delta}{R}\right)^\beta - \pi(BR + A(H-\delta))(H-\delta)w_a^e. \tag{3}$$

Equilibrium is reached when $(dE_{\rm Hg}/d\delta)_H = 0$, while the stability criterion requires $(d^2E_{\rm Hg}/d\delta^2)_H > 0$. This corresponds to a "fixed grip" configuration [4]. The resulting force ($k\delta$, obtained numerically) as a function of the base displacement H is plotted in Fig. 4(d) for different values of w_a^e. As H approaches zero, a real solution ceases to exist and the drop detaches from the surface. The force at this point is the force of adhesion $F_{\rm Ad}^{\rm Hg}$, and it is plotted as a function of w_a^e in the inset of Fig. 4(d). Using the values

for the parameters S, A, and B obtained for $\theta_p = 120°$, and $w_a^e = 1.82$ mJ/m^2, the force of adhesion predicted by our model is -0.6 μN, in good agreement with the experimental value of -0.5 μN [Fig. 1(l)]. We note that in the case of the contact with the flat surface (Fig. 1, left column), our model underestimates the force of adhesion by a factor of 1/3 ($F_{\mathrm{Ad}}^{\mathrm{Hg}} = -15$ μN if $\phi_s = 1$) since the pronounced deformation of the drop's profile demands different expressions for E_s and E_E than those of Eq. (3).

An analytical approximate solution of $(dE_{\mathrm{Hg}}/d\delta)_H = 0$ can be found if we impose $\beta = 2.5$, which still yields a reasonably good fit to E_E as obtained from Eq. (2) [11]. The force of adhesion then becomes

$$F_{\mathrm{Ad}}^{\mathrm{Hg}} = -B\pi R w_a^e. \tag{4}$$

Similarly, as in the contact of solids [Eq. (1)], $F_{\mathrm{Ad}}^{\mathrm{Hg}}$ is independent of the source of the restoring elastic force (γ_{lv}) and does not depend on the quadratic term A of the contact area. The percentual error between the approximate analytical and the exact numerical solutions is of the order of 2% [11]. This suggests that the whole force vs compression curve $F^{\mathrm{Hg}}(x)$ of the Hg drop can be recovered from the solution of Derjaguin's model multiplied by B, i.e., $BF^{\mathrm{Derj}}(x) \approx F^{\mathrm{Hg}}(x)$, when a compliant elastic solid is considered, characterized by an effective elastic constant given by $K \equiv 4/3\pi(k_1 + k_2)$ where $k_i \equiv (1 - \nu_i^2)/\pi E_i$ and ν_i and E_i are the Poisson's ratio and Young's modulus of each body i [3]. The corresponding contributions to the energy balance in Derjaguin's model are $E_E = (2/5)KR^3(x/R)^{5/2}$ and $E_s = w_a^e \pi a_0^2 = w_a^e \pi R^2 (x/R)$, giving a total energy

$$E_{\mathrm{Derj}} = \frac{k\delta^2}{2} + \frac{2}{5}KR^3\left(\frac{H-\delta}{R}\right)^{5/2} - \pi R(H-\delta)w_a^e. \tag{5}$$

Comparing with the equivalent expression for the Hg drop [Eq. (3)], a dimensional analysis shows that K must scale as $S\gamma_{\mathrm{lv}}/R$. Indeed, Fig. 4(e) shows that by setting $K = 55\pi S\gamma_{\mathrm{lv}}/R \approx 65$ kPa, the force curve obtained from the compression of the 350 μm Hg drop can be recovered by multiplying by B the corresponding reaction force of the deformed elastic solid. Despite the good match shown, this analogy would no longer be valid for $w_a^e > 5$ mJ/m^2 [11]. We note that the effective K used in the comparison of Fig. 4(e) is over 2 orders of magnitude smaller than that of the softest rubber, but it is comparable to the Young's modulus of biological cells [20]. This analysis along with the constancy of $F_{\mathrm{Ad}}^{\mathrm{Hg}}$ with respect to the preload plus the vanishment of the CAH, allows us to conclude that the dewetting of a liquid from a surface with very low interaction energy is equivalent to the detachment process of a solid. Based on this analogy we propose that this system would be ideal to investigate the dynamic formation and rupture of both weak and strong individual pinning points by monitoring the shift in resonant frequency of the fiber during the forced wetting of a macroscopic Hg drop, in a similar way that dynamic microwelding is probed on macroscopic gold spheres [12].

We acknowledge funds from DGAPA-UNAM: IN-104911, CJIC/CTIC/2135/ 2009 and CONACYT, 17767. We thank J. Cruz and M. Monroy for technical assistance.

*To whom correspondence should be addressed.
escobar@fisica.unam.mx

[1] B. V. Derjaguin, Kolloid-Z. **69**, 155 (1934).
[2] B. V. Derjaguin, V. M. Muller, and Y. P. Toporov, J. Colloid Interface Sci. **53**, 314 (1975).
[3] K. L. Johnson, K. Kendall, and A. D. Roberts, Proc. R. Soc. A **324**, 301 (1971).
[4] D. Maugis, J. Colloid Interface Sci. **150**, 243 (1992).
[5] E. Barthel, J. Phys. D **41**, 163001 (2008).
[6] P. G. de Gennes and F. Brochard-Wyart, *D. Quere: Capillarity and Wetting Phenomenae* (Springer, New York, 2002).
[7] J. F. Joanny and P. G. de Gennes, J. Chem. Phys. **81**, 552 (1984).
[8] M. Delmas, M. Monthioux, and T. Ondarcuhu, Phys. Rev. Lett. **106**, 136102 (2011).
[9] D. Bonn, J. Eggers, J. Indekeu, J. Meunier, and E. Rolley, Rev. Mod. Phys. **81**, 739 (2009).
[10] J. V. Escobar, C. Garza, J. C. Alonso, and R. Castillo, Appl. Surf. Sci. **273**, 692 (2013).
[11] See Supplemental Material at http://link.aps.org/supplemental/10.1103/PhysRevLett.111.226102 for experimental procedure and precisions on several issues.
[12] R. E. Johnson and R. H. Dettre, *Contact Angle, Wettability, and Adhesion*, Advances in Chemistry Series Vol. 43 (American Chemical Society, Washington, DC, 1964), p. 112.
[13] R. Budakian and S. J. Putterman, Appl. Phys. Lett. **81**, 2100 (2002).
[14] L. H. Lee, *Fundamentals of Adhesion* (Plenum, New York and London, 1991), p. 265.
[15] A. A. Griffith, Phil. Trans. R. Soc. A **221**, 163 (1921).
[16] J. Israelachvilli, *Intermolecular and Surface Forces* (Academic, New York, 1992).
[17] B. N. J. Persson and E. Tosatti, J. Chem. Phys. **115**, 5597 (2001).
[18] A. B. D. Cassie and S. Baxter, Trans. Faraday Soc. **40**, 546 (1944).
[19] H. Hertz, J. Reine Angew. Math. **1882**, 156 (2009).
[20] T. G. Kuznetsova, M. N. Starodubtseva, N. I. Yegorenkov, S. A. Chizhik, and R. I. Zhdanov, Micron **38**, 824 (2007).